^{1}H NMR study of the magnetic properties and electronic structure of the hydroxide complex of substrate-bound heme oxygenase from *Nesseria meningitidis*; Influence of the axial water deprotonation on the distal H-bond network

*Li-Hua Ma[†], Yangzhong Liu[†], Xuhang Zhang[‡], Tadashi Yoshida[‡] and Gerd N. La Mar [†]**

Supporting Information

Four figures (partially relaxed spectra for *Nm*HO-PH-OH, Curie plot for heme methyls and comparison of magnetic axes determination for *Nm*HO-PH-CN with and without considerations of rhombic anisotropies, and labile proton saturation factors) and one Table (chemical shifts for assigned *Nm*HO-PH-OH residues), total 5 pages.

Table S1. Observed chemical shifts for assigned residues in *Nm*HO-PH-OH[a]

		δ_{DSS}(obs)
Ala12	$C_{\alpha}H$	3.39
	$C_{\beta}H_3$	1.24
Leu15	$C_{\delta1}H_3$	-0.60
Thr20	$C_{\gamma}H_3$	1.30
Ala21	$C_{\beta}H_3$	1.47
Val22	$C_{\gamma1}H_3$	0.70
	$C_{\gamma2}H_3$	0.98
Asp24	$C_{\beta1}H$	2.82
	$C_{\beta2}H$	3.08
Phe52	$C_{\alpha}H$	4.40
	$C_{\beta1}H$	3.03
	$C_{\beta2}H$	3.13
	$C_{\varepsilon}Hs$	7.43
	$C_{\zeta}H$	7.31
His53	$C_{\delta1}H$	7.45
	$C_{\varepsilon2}H$	7.95
Tyr112	$C_{\beta1}H$	3.02
	$C_{\beta2}H$	3.30
	$C_{\delta}Hs$	6.90
Cys113	$C_{\beta1}H$	2.72
	$C_{\beta2}H$	2.76
Ala114	$C_{\alpha}H$	4.37
	$C_{\beta}H_3$	1.90
Asn118	$C_{\beta1}H$	3.12
	$C_{\beta2}H$	3.02
Ala121	$C_{\beta}H_3$	2.30
Phe125	$C_{\delta}Hs$	7.04
	$C_{\varepsilon}Hs$	7.12
	$C_{\zeta}H$	7.20
Ala139	$C_{\alpha}H$	4.11
His141	$C_{\delta2}H$	6.30
	$C_{\varepsilon1}H$	7.60
Leu142	$C_{\delta2}H_3$	0.80
	$C_{\gamma}H$	0.05
Asn147	$C_{\alpha}H$	4.15
	$C_{\beta1}H$	1.42
	$C_{\beta2}H$	1.96
Trp153	$C_{\delta1}H$	6.95
Val157	$C_{\alpha}H$	2.85
	$C_{\beta}H$	1.55
	$C_{\gamma1}H_3$	0.37
	$C_{\gamma2}H_3$	-0.02
Ala180	$C_{\alpha}H$	2.58
	$C_{\beta}H_3$	0.58
Phe181	$C_{\beta1}H$	3.57
	$C_{\beta2}H$	3.03
Ala182	$C_{\alpha}H$	4.10
	$C_{\beta}H_3$	1.66
Phe183	$C_{\alpha}H$	4.53
	$C_{\beta1}H$	3.68
	$C_{\beta2}H$	3.42
	$C_{\delta}Hs$	7.64
	$C_{\varepsilon}Hs$	7.37
Tyr184	$C_{\delta}Hs$	6.18
	$C_{\varepsilon}Hs$	6.48
Val186	$C_{\alpha}H$	3.64
	$C_{\beta}H$	2.40
	$C_{\gamma2}H_3$	1.25
Val187	$C_{\alpha}H$	3.42
	$C_{\beta}H$	1.50
	$C_{\gamma1}H_3$	0.69
	$C_{\gamma2}H_3$	0.08

a) δ_{DSS}(obs) in ppm referenced to DSS via the solvent resonance, in ^2H_2O at pH 9.1, 100 mM bicarbonate at 25°C.

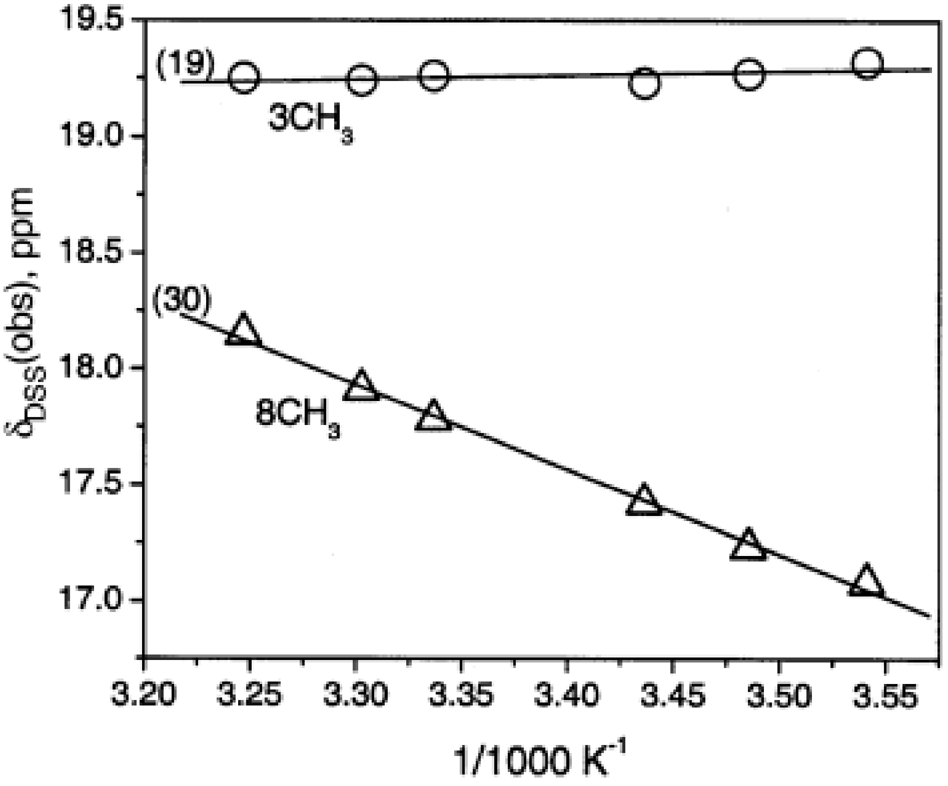

Figure S1. Curie plot (^{1}H NMR δ_{DSS}(obs) versus reciprocal absolute temperature (T^{-1})) for the resolved heme methyl peak for *Nm*HO-PH-OH at pH 10.5, in ^2H_2O, 100 mM bicarbonate at 25°C. The apparent intercepts, in ppm, at $T^{-1} = 0$, are given in parenthesis.

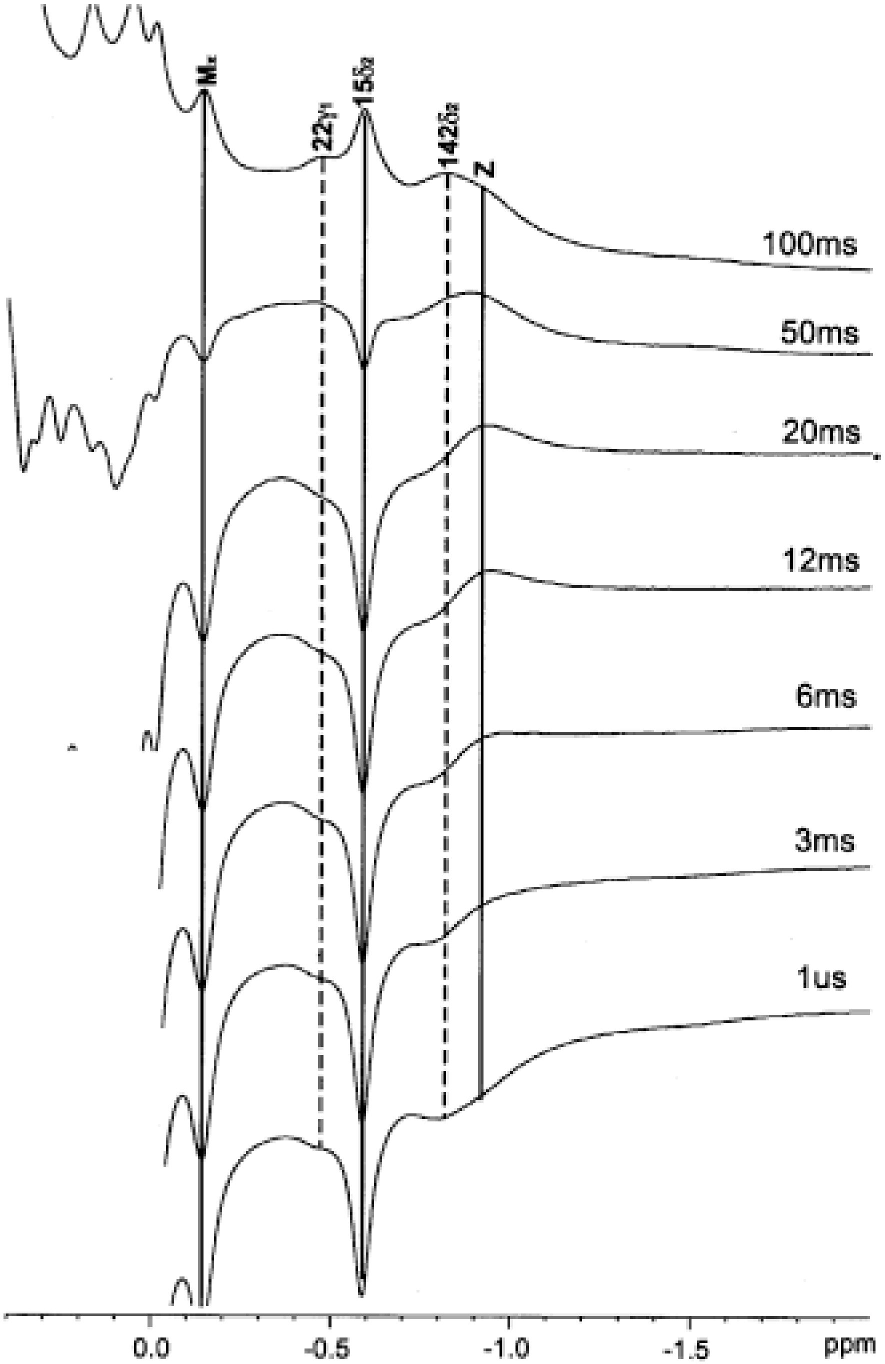

Figure S2. Partially relaxed spectra in an inversion-recovery pulse sequence for the resolved upfield 600 MHz ^1H NMR spectrum of *Nm*HO-PH-^2H_2O in ^2H_2O 100 mM bicarbonate, pH 10.5 at 25°C. The relaxation delay times are given on the right. Peaks are labeled by amino acid number and proton position, with solid and dashed lines representing signals in *Nm*HO-PH-OH and *Nm*HO-PH-H_2O, respectively. The single proton peak z exhibits a null at ~5 ms, or a T_1 ~8 ms, and exhibits the shift [38, 49] and T_1 are consistent with it arising from a vinyl H_β.

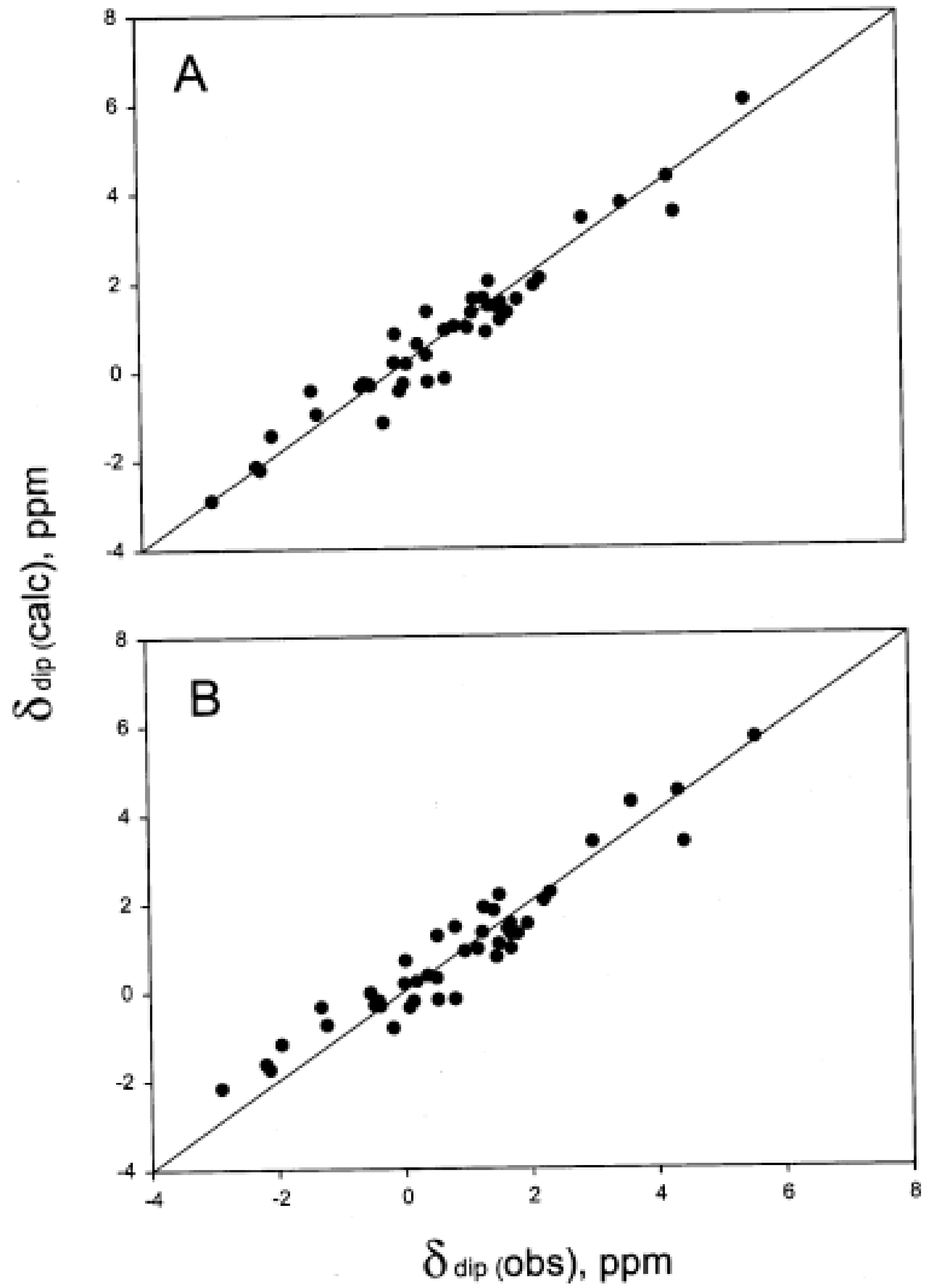

Figure S3. Plots of δ_{dip}(obs) versus δ_{dip}(calc) obtained from the magnetic axes determination of *Nm*HO-PH-CN based on: (**A**) five-parameter search to determine $\Delta\chi_{ax}$ (= 2.48 ± 0.1 x 10^{-8} m^3/mol), $\Delta\chi_{rh}$ (= -0.52 ±0.09 x 10^{-8} m^3/mol), the tilt of magnitude (β = 8±1°), tilt direction (α = 280 ± 10°) and rhombic axes (κ = 41 ± 10°); and a three-parameter search keeping $\Delta\chi_{rh} = 0$ and $\gamma = 0$, to determine $\Delta\chi_{ax}$ (=2.4 ±0.1 x 10^{-8} m^3/mol), tilt magnitude (β = 4±1°) and tilt direction (α = 260±10°). The residues error function, F/n, is smaller for the five-parameter (F/n = 0.05) than three-parameter (F/n = 0.06) search.

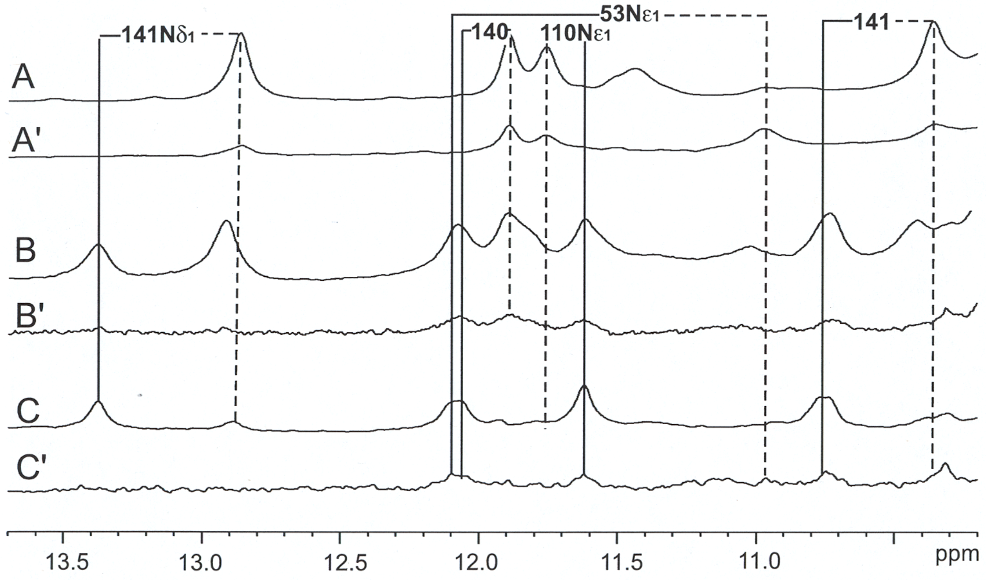

Figure 4S. 3:9:19 reference spectra [52] for the labile proton involved in strong H-bonds in *Nm*HO-PH-H_2O/*Nm*HO-PH-OH mixture in ^1H_2O, 50 mM in phosphate at 25°C, as a function of pH. Assigned peak in *Nm*HO-PH-H_2O [50] and *Nm*HO-PH-OH are connected by bars over the reference spectra, with dashed and solid vertical lines representing the *Nm*HO-PH-H_2O and *Nm*HO-PH-OH complexes, respectively. (**A**) pH 7.2 (~98% *Nm*HO-PH-H_2O/2% *Nm*HO-PH-OH) (**B**) pH 9.4 (~60% *Nm*HO-PH-H_2O/~40% *Nm*HO-PH-OH) and (**C**) pH 10.2 (20% *Nm*HO-H_2O/80% *Nm*HO-OH). Magnetization difference 3:9:19 traces upon subtracting the off-resonance from the on-resonance saturation of the water signals as a function of pH as shown in A', B' and C', which demonstrate the saturation factor due to exchange and not increased (for His141 $N_\delta H$ actually decreased) upon increasing pH from 7.2 to 10.2.